REPORT ON THE Characterization of the Adherence of Plasma-Sprayed ZrO_2 Coatings

P. F. Becher and R. W. Rice
Naval Research Laboratory
Washington, D. C. 20375

INTRODUCTION

Coatings consisting of ceramic materials have received considerable attention for use in severe thermal and corrosive environments such as those exhibited in turbine[1] and coal gasification[2] units. While such areas as corrosion, erosion or thermal fatigue must be considered in the use of such coating, the initial critical issue is often adherence. Previous studies have shown that the level of adherence of thick film systems[3-5] and ceramic joints formed by solid state bonding[6] is often very dependent upon the microstructure adjacent to, or within, the interface region. The role of material properties (and microstructure) in ceramic coating adherence has also been discussed together with effects of residual coating stresses, interface (particularly that associated with the ceramic layer), and fracture toughness in the ceramic.[7] Furthermore the composition and amount of the metal bond coat used as an intermediate layer between the ZrO_2 coating and substrate can strongly influence adherence.[8,9] Along this same line, it has also been suggested that the inclusion of a chromium layer beneath the ZrO_2 layer might alleviate fracturing in

DISCLAIMER

the ZrO_2 coating upon exposure to hot corrosive gases,[10] i.e. in a manner similar to self-healing coatings where the chromium oxidizes[11]. Such findings point to the need to characterize the composition and microstructure of ceramic coating systems and to correlate these with measurements of coating adherence to gain an understanding of how adherence might be optimized. The present study has thus examined ZrO_2 coating of various compositions (i.e. Y_2O_3 and MgO stabilizers) phase content (i.e. cubic, tetragonal, and monoclinic) and differing metallic interlayers.

EXPERIMENTAL

The materials tested included flat substrates coated first with various bond coats then plasma sprayed with various ZrO_2 composition, Table I. Microstructure and composition (element distribution via energy dispersive x-ray analysis) were characterized on polished cross sections of the coatings, along with fractographic (i.e. locus of failure) analysis using standard scanning electron microscopy. X-ray diffraction analysis was employed on the as-sprayed surfaces of and fracture surfaces in the ZrO_2 coatings to determine phases present The tests for coating adherence included both a fracture mechanics tests and a tensile pull test. The latter employed a square cross section coated sample cut from the coupons supplied. For the purposes of the tensile test a threaded brass block was attached to the ZrO_2 coating using an adhesive.* The substrate was held in a grip and the load

*Adhesive-Bondmaster M777, National Starch and Chemical Corp., Bridgewater, N. J.

applied normal to the coating/substrate interface by a threaded coupling attached to the cross head of the test machine, Figure 1. The fracture toughness (K_{IC}) of the coatings was determined using a modification[12] of the applied moment[13] double cantilever beam configuration,[13] Figure 2. Both measurements were made at 22°C, 40% relative humidiy and a loading rate of 0.5 cm/min. in an Instron test machine with a modified load train in corporating gas floated spherical air bearings to minimize parasitic bending moments.[14]

RESULTS

The ceramic coatings tested involved a wide variety of starting powder (Table I) which resulted in the presence of various amounts of non-cubic ZrO_2. This variation ranges in the coatings, listed in Table I, from 100% cubic to predominately noncubic, ZrO_2. Microstructures of these same coatings observed on fractured cross sections all exhibit very similar features in the ZrO_2 layer, Figure 3. These features consist of plate-like ZrO_2 regions (10-15 microns across x 1-3 microns thick) formed when the melted (or partially melted) particles struck the surface of the sample being coated. Fractures through these plates suggest that they consist of fine ($\sim$0.5 micron diameter) columnar grains. In addition, the ZrO_2-MgO coatings, of course, contain MgO regions as these coatings actually consist of two different chemical phases (i.e. MgO and ZrO_2, Table 1).

Element maps of polished cross sections of the coatings, Figure 4, illustrate two features which differentiated to sources of coatings, Table I. First note that the bond coat in the ZrO_2 coated samples from Source I is thinner and has a very uniform thickness. Second the coatings from Source II have highly interlocking interfacial structures at the substrate-bond coat and bond coat-ZrO_2 layer interfaces. While the coated samples from Source I have some interlocking interfacial structure at the ZrO_2-bond coat interface, but the degree of interlocking appear less than the coatings from Source II. Furthermore, the bond coat-substrate interface appears quite smooth in the coated samples from Source I.

The room temperature adherence values of the various coatings where a crack is propagated parallel (or nearly so) to the the plane of the coating to substrate interface are listed in Table I. Note that the adherence strength of the fully cubic ZrO_2 coatings (from both Source I and II, Table I) are somewhat lower than measured earlier on very similar coatings.[9] This is felt to reflect the damage introduced by having to machine samples from the coated coupon specimens in the current tests as opposed to testing samples where the coatings were applied to specimens of the geometry to be used in testing.[9] On the other hand, K_{IC} values for ZrO_2-MgO coatings of 1.0 to 1.5 MPa-$m^{1/2}$ have been obtained by the single edge notched beam method.[14]

These are comparable to the values obtained here with differences in both testing and processing (spraying) conditions likely being the cause for the small difference in K_{IC} values obtained in that study versus the current work.

Of the ~ 0.05 cm thick ceramic coatings listed in Table I, those containing both cubic and non-cubic ZrO_2 phases appear to exhibit improved adherence in terms of both higher strengths and fracture toughness values over the fully cubic ZrO_2 coatings. This is true despite the fact those coatings containing non-cubic ZrO_2 incorporate: 1) a different substrate material, and 2) a thicker (as well as a different) bond coat layer than one of the cubic ZrO_2 coated samples. Finally the addition of a thin chromium layer between the ZrO_2 and bond coat had negligible effect on adherence.

DISCUSSION

The adherence of plasma sprayed ZrO_2 coatings at low temperatures (i.e. near room temperature) appears to be enhanced by several features: 1) the formation of a distinct interlocking interface structure, and 2) incorporation of MgO and some noncubic ZrO_2 within the cubic ZrO_2 layer. While at this time it is difficult to fully determine the sources of adherence, several comments are in order.

First it must be recognized that there are the underlying effects of residual stresses generated during the plasma spraying process. This is indicated by the thick-

ness dependence of adherence strength observed in one of the cubic ZrO_2 coatings (Table I). It is also suggested by the greater adherence in the MgO containing ZrO_2 coatings where the MgO exists as a second phase (Table I). In this case the MgO regions can plastically deform during cool down of the coating after the spraying process, and thus relieve a greater portion of the stresses generated than in the case of the Y_2O_3 stabilized ZrO_2 coatings. In fact, it should be noted that the fracture path within the ZrO_2 layer in the more adherent coatings tended to be located further away from the ZrO_2-bond coat interface as the adherence increased. Residual stresses which are generated by the mismatch in thermal expansion between the ZrO_2 and bond coat/substrate alloys would be concentrated at the ZrO_2-bond coat interface. Thus, relief of residual stresses should not only improve adherence but also shift the locus of failure away from the interface, as observed.

It should be remembered also that the fracture path will not follow along the exact bond coat-ZrO_2 interface except for very smooth interfaces. Crack deflections required to follow an interlocking interface would require more energy than a more planar fracture path. [Such increases in the energy to propagate a crack (i.e. increases in K_{IC}) by forcing it to attempt to propagate along an interlocking interface have been observed in a thick film systems.[15]] Thus fracture will involve a mixture of frac-

ture along the interface and through the ZrO_2 with interlocking interface. Such mixed fracture, in fact, is observed in the fracture (or spalling) of many ZrO_2 coatings.

Noncubic ZrO_2 in the ZrO_2 layer appears to increase the coating adherence. This is indicated by the increase in adherence as the amount of tetragonal phase increases from 0% to $\sim$70% in the coatings listed in Table I. While part of this increased adherence is due to the presence of an MgO phase, amongst those ZrO_2 coatings containing MgO there is a further increase in adherence with increase in tetragonal/monoclinic ZrO_2 content. This indicates that some strengthening (and/or toughening) effects are being derived by the inclusion of the noncubic phases. This may result either from pre-existing microcracking due to the presence of monoclinic ZrO_2 or from the toughening associated with the tetragonal to monoclinic transformation as a result of the applied mechanical stresses.[16,17]

In the absence of chemical bonding across the interface, a strong mechanical bond needs to be established at the interface. Some chemical bonding is possible with plasma spraying but the short times at temperature apparently limit the formation of such a bond. For those cases where high strengths and stresses normal to the interface are critical enhancing the chemical bonding nature of the interface ought to be examined (e.g. possibly post spraying anneals could be used to enhance the chemical bond

via diffusion or reactions). The current coatings heavily rely on a mechanically interlocked interface to raise the ceramic coating adherence. This becomes more apparent in the more adherent coatings where failure occurs well within the ZrO_2 layer and not at the ceramic-bond coat interface.

SUMMARY

Analysis of the microstructure and adherence of ZrO_2 coatings revealed that the adherence decreased with increasing coating thickness and could be increased by incorporating MgO as a second phase as well as by including noncubic ZrO_2 in the cubic ZrO_2 coating. Residual stresses from the plasma spraying process limit adherence (hence the coating thickness dependence) but these can be relieved by plastic flow in the MgO phase during post-spray cooling. Some degree of strength/toughening is also derived by the presence of microcracks and/or from transformation associated with the presence of tetragonal ZrO_2.

ACKNOWLEDGEMENTS

The assistance of S. R. Levine of NASA-Lewis and I. Kvernes of the Central Institute for Industrial Research, Oslo, Norway in obtaining coated samples and R.Carmen of NRL in carrying out the adherence tests are gratefully aknowledged. The work was supported by the Department of Energy under Interagency Agreement No. DE-AI03-78ET15328.

REFERENCES:

1. L. T. Shiembob, Development of a plasma-sprayed ceramic gas path seal for high pressure turbine applications. Lewis Research Center, NASA Final Rept., 1977, Pratt and Whitney Aircraft Group, East Hartford, Conn. Contract NA53-19759.

2. R. Swaroop, Ceramic coatings for components exposed to coal-gas environments: a review, Argonne Natl. Lab. Pub. ANL-76-124, 1976.

3. P. F. Becher and W. L. Newell, "Adherence-fracture energy of a glass-bonded thick-film conductor: effect of firing conditions," J. Mater. Sci. 12, 90-96 (1977).

4. P. F. Becher, "Fritted thick film conductor adherence fracture energy: influence of alumina substrates," ibid., 1088-1094 (1978).

5. P. F. Becher, "Fritted thick film conductor adherence: role of firing atmosphere," ibid., 13, 457-459 (1978).

6. P. F. Becher and S. A. Halen, "Solid-state bonding of Si_3N_4," Am. Ceram. Soc. Bull. 58 [6] 582-583 (1979).

7. P. F. Becher, R. W. Rice, C. Cm. Wu, and R. L. Jones, "Factors in the degradation of ceramic coatings for turbine alloys," J. Thin Solid Films 53 225-232 (1978).

8. S. Stecura, Effects of yttrium, aluminmum and chromium concentrations in bond coatings on the performance of zirconia-yttria thermal barriers, NASA Tech Memo NASA-TM-79206 (1979).

9. S. R. Levine, Adhesive/cohesive strength of a ZrO_2 12 w/o Y_2O_3/NiCrAlY thermal barrier coating, NASA Tech Memo, NASA TM-73792 (1978).

10. I. Kvernes and P. Fartum, "Use of corrosion resistant plasma sprayed coatings in diesel engines," J. Thin Solid Films, 53, 259-269 (1978).

11. G. Perugini, "Ceramic self-sealing coatings for high-temperature surfaces," Ceramurgia Inter. 4 (1) 3-13, (1978).

12. P. F. Becher, W. L. Newell and S. A. Halen, in Fracture Mechanics of Ceramics, Vol. 3, pp. 463-471, R. C. Bradt, D. P. H. Hasselman and F. G. Lange (eds.), Plenum Publ. Corp., NY (1978).

13. S. W. Freiman, D. R. Mullville and P. W. Mast, "Crack Propagation Studies in Brittle Materials," J. Mater. Sci. 8 [11] 1527-33 (1973).

14. M. H. Leipold and P. G. Becher, A mechanical tension testing facility for brittle materials, NASA Tech Rep 32-1179, Jet Propulsion Laboratory, Oct. 1967.

15. I. Kvernes, Development and engine testing of coatings on diesel engine components, DOE Prog. Rep., Contract No. ET-78-X-01-4288, Central Inst. for Industrial Res., Oslo, Norway, Jan. 1980.

16. W. D. Bascom, P. F. Becher, J. L. Bitner and J. S. Murday, in Adhesion measurement of thin films, thick films and bulk coatings (ASTM STP 640) pp. 63-81, K. L. Mittal (ed.) ASTM, Philadelphia (1978).

17. R. C. Garvie, R. H. J. Hannink, R. R. Hughan, N. A. McKinnon, R. T. Pascoe and R. K. Stringer, "Strong and tough partially-stabilized zirconia ceramics," J. Aust. Ceram. Soc. 13 (1) 8-11 (1977).

18. N. Claussen, J. Steeb and R. F. Pabst, "Effect of induced microcracking on the fracture toughness of ceramics, Am. Ceram. Soc. Bull., 56 (6) 559-562 (1977).

ADHERENCE OF PLASMA SPRAYED ZrO_2 COATINGS

Sample	Composition wt %	ZrO_2 Layers Phases in wt %	ZrO_2 Layers Thickness cm	Bond Layer(s) Composition wt %	Bond Layer(s) Thickness cm	Tensile Strength MPa	K_{IC} MPa/m3/2	Locus of Failure
Coatings on FeCrNi Alloy Substrates+8	ZrO_2+25MgO	70% t 25% c 10% m with 10%MgO	0.04	Ni20Cr6Al		5.00±0.35	2.7±0.5	Within ZrO_2 layer
9	same	same	same	Cr / Ni20Cr6Al	0.004 / 0.010	5.35±0.30	2.9±0.2	In or near to ZrO_2 to bond coat interface
7	ZrO_2+24MgO	45% t	0.04-0.05	Cr / Ni20Cr6Al	0.004 / 0.010	4.00±0.25	2.2±0.1	Same: Cr found on fracture surface
4	same	same	same	Ni20Cr6Al	0.010	4.50±0.10	2.4±1.0	In ZrO_2 layer
5	ZrO_2+20Y_2O_3	90% c 10% m	0.04	Ni20Cr6Al	0.010	3.05±0.45	1.7±0.9	Near ZrO_2 to bond layer interface
6	same	same	same	Cr / Ni20Cr6Al	0.004 / 0.010	3.45±0.60	1.6±0.3	same
Coatings on NiCrCo Alloy Substrates++	ZrO_2+12Y_2O_3	100% cubic	0.05	Ni16Cr56Al06Y	0.005	2.50±0.60	1.9±0.9	Near ZrO_2 to bond layer interface

+Supplied by Central Institute for Industrial Research, Oslo, Norway; Metco ZrO_2 powders used for all except 8 and 9 which used Castoline powders, Metco NiCrAl powder used for bond coat.

++Supplied by NASA-Lewis, Cleveland, Ohio.

*t-tetragonal; m-monoclinic; c-cubic ZrO_2 phases.

FIGURE CAPTIONS

Fig. 1. Tensile Paull Test for Ceramic Coated Substrates. The coated samples are machined from large coupons with subsequent tensile load applied via a brass coupling block epoxied to the coating surface.

Fig. 2. Test for Determining K_IC Values for Adherence Of Ceramic Coatings to Substrate. The specimen used for coated substrates deviates from that used in K_IC test of bulk materials[13] by the fact that half of DCB specimen consists of a brass arm (2 in figure) attached to the coating[3] on the substrate (1) by epoxy. This requires that the specimen geometry be altered so that there is equal strain energy in each half of the DCB specimen (i.e. as indicated by $E_1I_1-E_2I_2$ where E is Youngs modulus and I is the moment of inertia of each half of the DCB specimen). Also, the applied moment to each arm must be constant therefore the applied load P/2 and the fulcrum point to coating surface (sample mid-plane) distance for each half of the DCB specimen must be equal. These considerations allow one to propagate a crack in the ZrO_2 coating with the crack plane parallel to the coating surface.

Fig. 3. Fracture Surface Microstructure of ZrO_2 Coatings. Fracture surfaces obtained from applying bending load parallel to coating surface to obtain a cross sectional view of coatings from Source I.

Fig. 4. Element Distribution of Polished Cross Sections of Cubic ZrO_2 Coated Samples from Sources I(A) and II(B).

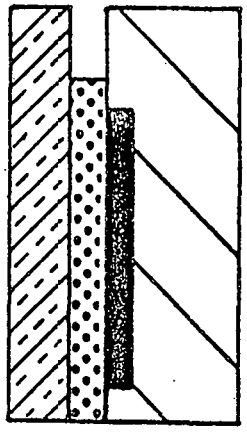

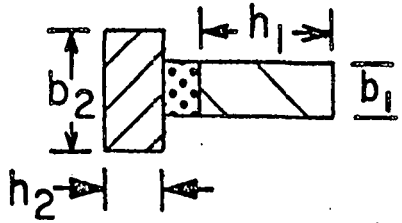

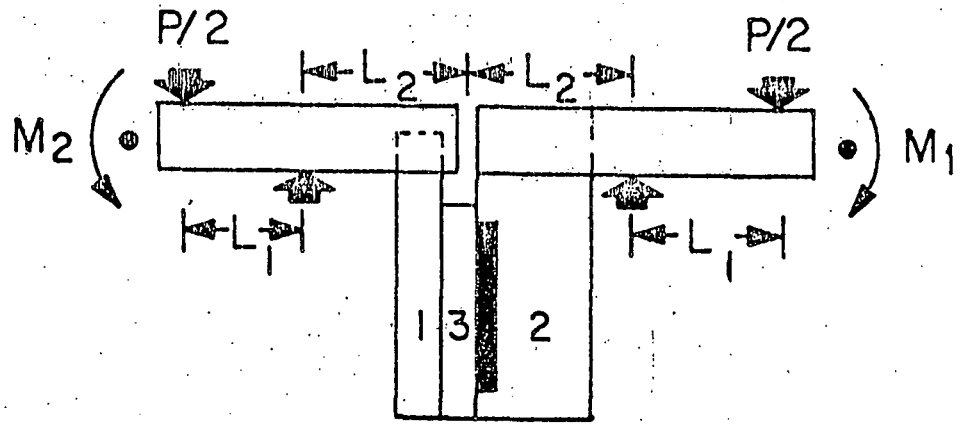

$$M_1 = M_2$$

$$E_1 I_1 = E_2 I_2$$

$$\frac{E_1 b_1 h_1^3}{12} = \frac{E_2 b_2 h_2^3}{12}$$

$$K_{Ic} = \frac{PL_1}{2}\left[\frac{6E_3}{b_1}\left(\frac{1}{E_1 I_1} + \frac{1}{E_2 I_2}\right)\right]^{1/2}$$

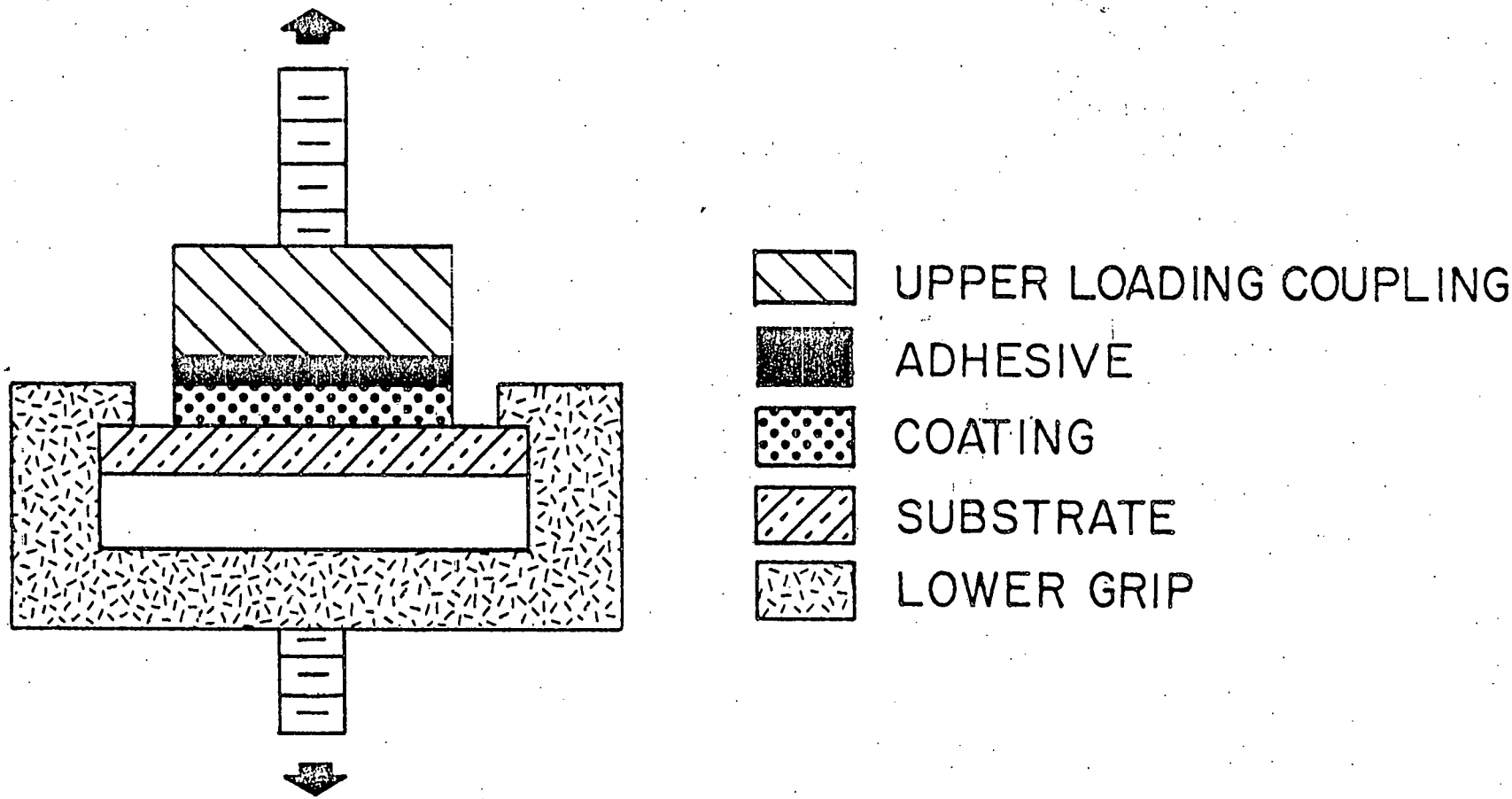
UPPER LOADING COUPLING
ADHESIVE
COATING
SUBSTRATE
LOWER GRIP

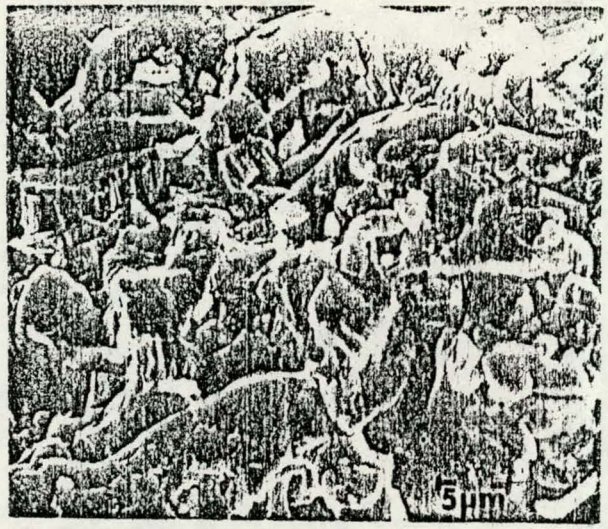

C 8 70T, >20C, <10M

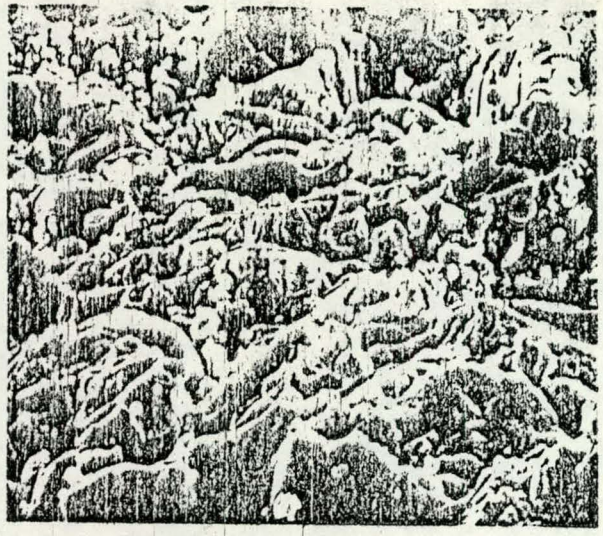

C 5 90T, 10M

C 7 45T, 55C, 5M

ZrO_2 Coatings

Fractured in Bending

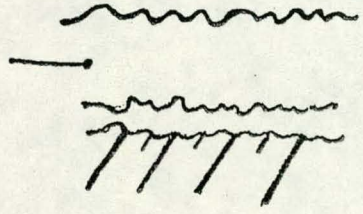

T Tetragonal
C Cubic
M Monoclinic

} ZrO_2

A

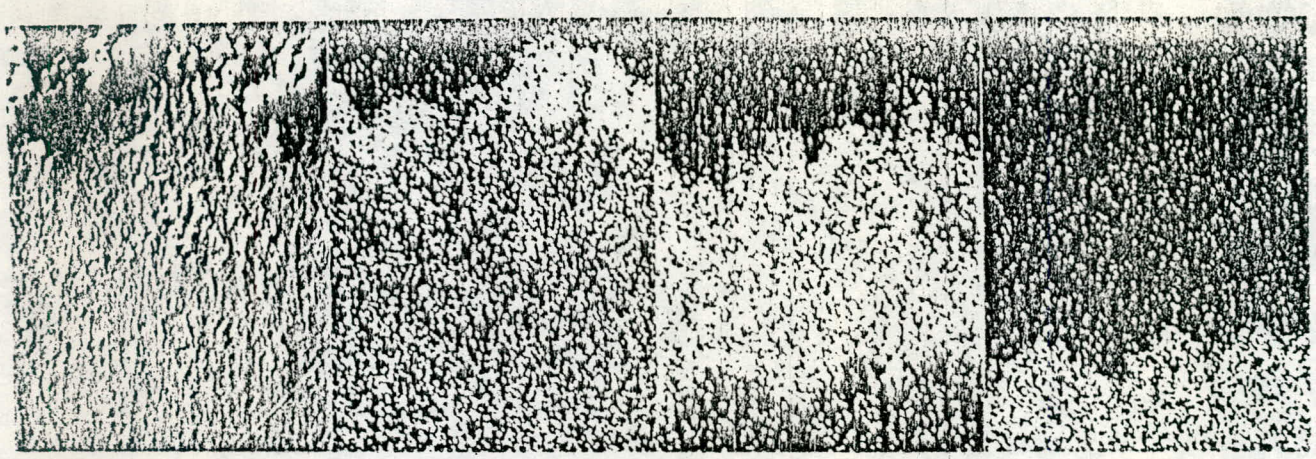

Cr Ni Fe

B

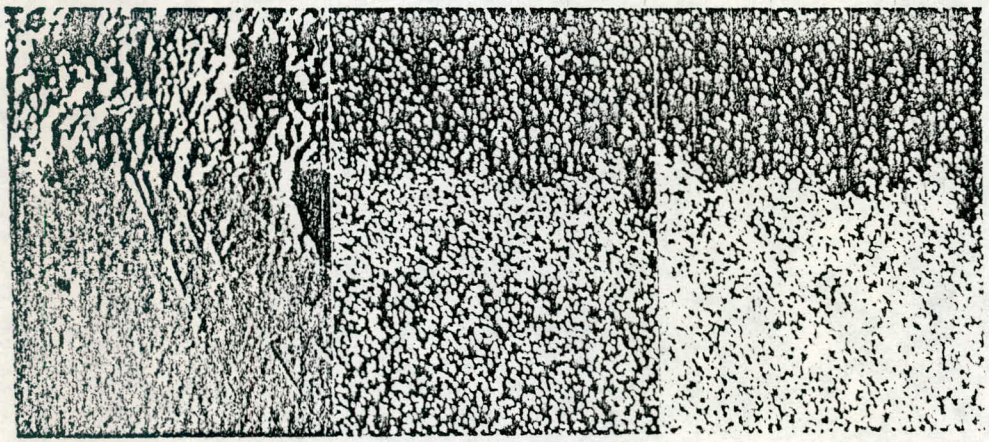

Cr Ni

ZrO_2

Bond Coat

Substrate

X-Ray Element Maps